XMM-Newton CCF Release Note

XMM-CCF-REL-167

PSF of the X-ray telescopes

A.M. Read

16 June 2004

1 CCF components

Name of CCF	VALDATE	List of Blocks changed	CAL VERSION	XSCS flag
XRT1_XPSF_0007.CCF	2000-01-01	KING_PARAMS		NO
XRT2_XPSF_0007.CCF	2000-01-01	KING_PARAMS		NO
XRT3_XPSF_0006.CCF	2000-01-01	KING_PARAMS		NO

2 Changes

New analysis has refined the values stored in the King function parameterisation of the 3 EPIC telescope point spread functions (PSFs), i.e. XRT1, XRT2 & XRT3. They are stored in the KING_PARAMS extension of the CCF, and are tabulated as functions of ENERGY and THETA (off-axis angle).

This analysis has dealt with purely on-axis sources, and the on-axis King parameters have been updated accordingly. The off-axis behaviour previously observed has been used to extrapolate the new on-axis parameters to new projected off-axis values.

3 Scientific Impact of this Update

The PSF is described by a King function whose parameters, core radius r_0 and index α, are themselves functions of energy and off-axis angle:

$$PSF_{\rm King}(r) = \frac{A}{(1+(\frac{r}{r_0})^2)^{\alpha}}$$

Earlier work [1, 2, 3] used many bright point sources both on and off axis to determine the energy dependent PSF. This resulted in a linear dependency of r_0 and α with energy and

off-axis angle. It is shown here that this linear dependency is not valid – the dependencies of r_0 and α are seen to be flatter (almost constant) with energy (at least out to $\sim 8-10\,\mathrm{keV}$).

3.1 Scientific Impact: Analysis and Results

The present analysis has made use of a small number of newer datasets that have become available, involving very long and clean observations (with few, if any, periods of high-background flaring) of very bright on-axis point sources. The data have all been taken in small window mode, such that these very bright sources are not significantly piled-up. Specifically, the most useful targets that have been used are listed (together with their revolution numbers) as follows:

MCG-06-30-15 (Revs. 301, 302, 303 [each $\sim 100\,\mathrm{ks}$])

Ark120 (Rev. 679, [$\sim 100\,\mathrm{ks}$])

3C273 (Revs. 94, 95, 96, 277, 370, 373, 472, 554, 563 [various exposures, just MOS])

Two threads of analysis were followed: One involved the forming of narrow-energy-band images from the brightest of these sources, and fitting the surface brightness radial profiles obtained from these images with a King function to obtain r_0 and α as a function of energy. A second analysis thread involved the extraction of spectra from narrow annuli around each point source, and once ARF files had been generated (this involving the actual form of the PSF), the spectra were fitted with standard spectral models, to see how (if at all) the spectral parameters obtained varied with extraction radius (for a point source of course, they should not vary at all). This whole process was repeated for several sets of PSF parameters (including those obtained from the surface brightness radial profile fitting described above).

In forming the narrow-band images, the MCG-06-30-15 data were predominately used. The datasets were first cleaned of times of high background, and FLAG=0 single-event images were created in X/Y coordinates (rather than RAWX/RAWY or DETX/DETY coordinates), to take into account effects of any small attitude shifts. Different energy binnings were used to get better statistics in the different energy bands for the radial fitting (hence the CCF parameters are now mapped to different energy values than in previous versions).

Before constructing the radial surface brightness profiles, the centre of the emission was found for each image via Gaussian fitting. The very small (and probably non-significant) shifts in Gaussian centre with energy were taken into account in constructing the radial profiles, which were then fitted with a King function. Two examples of surface brightness radial profiles plus fitted King profiles are shown in Fig.1.

This resulted in r_0 and α values for 10 different energies, for the three different instruments and for the three MCG-06-30-15 observations. Exposure-weighted mean values (over the

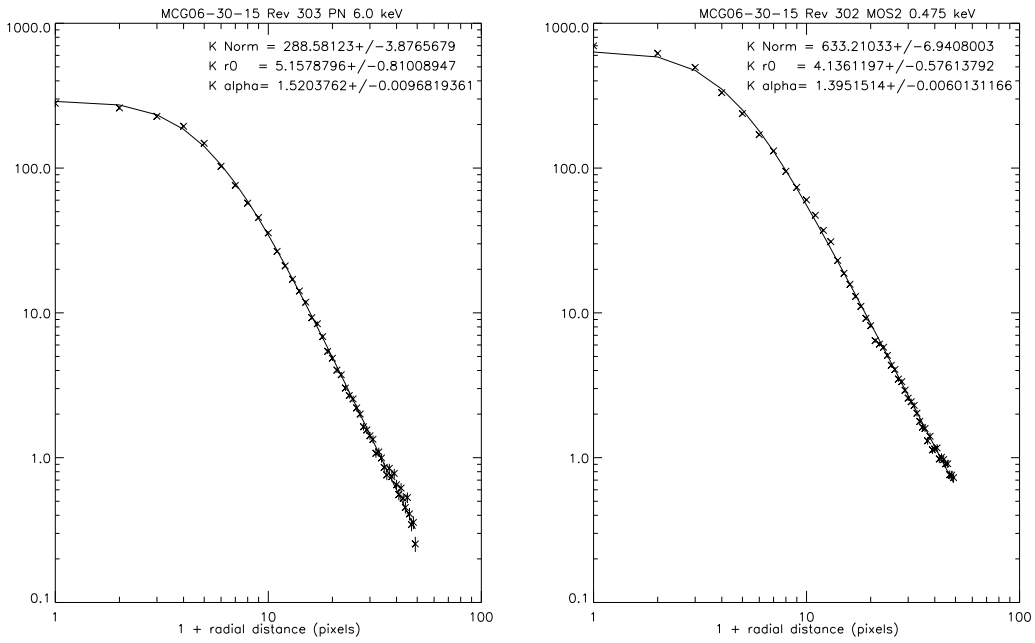

Figure 1: Surface brightness radial profiles (crosses) plus fitted King profiles (lines) for two examples: (left) MCG-06-30-15 Rev. 303 pn at 6 keV and (right) MCG-06-30-15 Rev. 302 MOS2 at 0.475 keV

three different observations) for r_0 and α were then calculated for each instrument and energy band. A separate analysis involving the 'stacking' of the separate relevant images from the different observations on top of one another, prior to the radial profile fitting, produced almost identical results to the values obtained via calculating the exposure-weighted mean values.

3.2 Scientific Impact: Application

The resultant dependencies of r_0 and α are seen to be flatter (almost $\sim$constant) with energy, at least up to $\sim 8-10\,\mathrm{keV}$ (where the $r_0 - E$ and $\alpha - E$ relationships turn over) than in the previous parameterization of the PSFs. This is shown in Fig. 2.

The new PSFs were used in the analysis of spectra extracted from narrow concentric annuli around a number of bright point sources, as described above. Fig.3 shows how the fitted normalization and power-law index vary as a function of extraction 'radius' (a circle of $0-5''$, then annuli of $5-10''$, $10-15''$, $15-20''$etc.) for the current CCF PSFs and the new CCF PSFs described here, for the MCG-06-30-15 Rev. 302 data. A point source, of course, should show no variation in fitted spectral parameter whether the spectrum is extracted from the very centre of the distribution or from the wings, but usage of the current PSFs result in a very wide range in spectral parameters for different radii. Usage of the new PSFs gives rise to a very significantly improved situation, with the fitted normalization and power-law index remaining constant and 'flat' with radius. Fig.4 shows

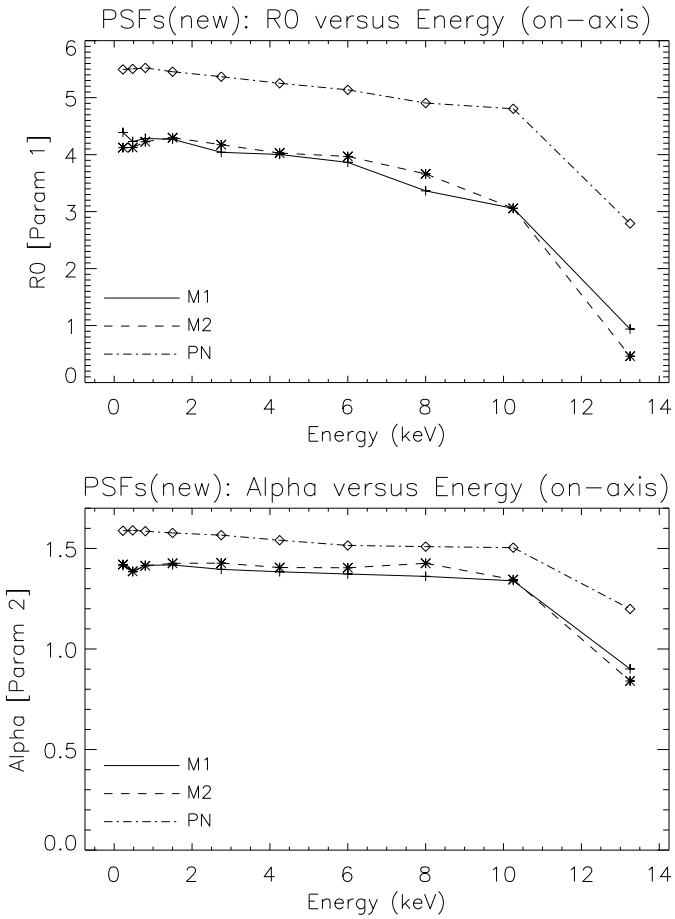

Figure 2: (top) r_0-Energy and (bottom) $\alpha-$Energy dependencies for the new MOS1, MOS2 and pn on-axis PSFs.

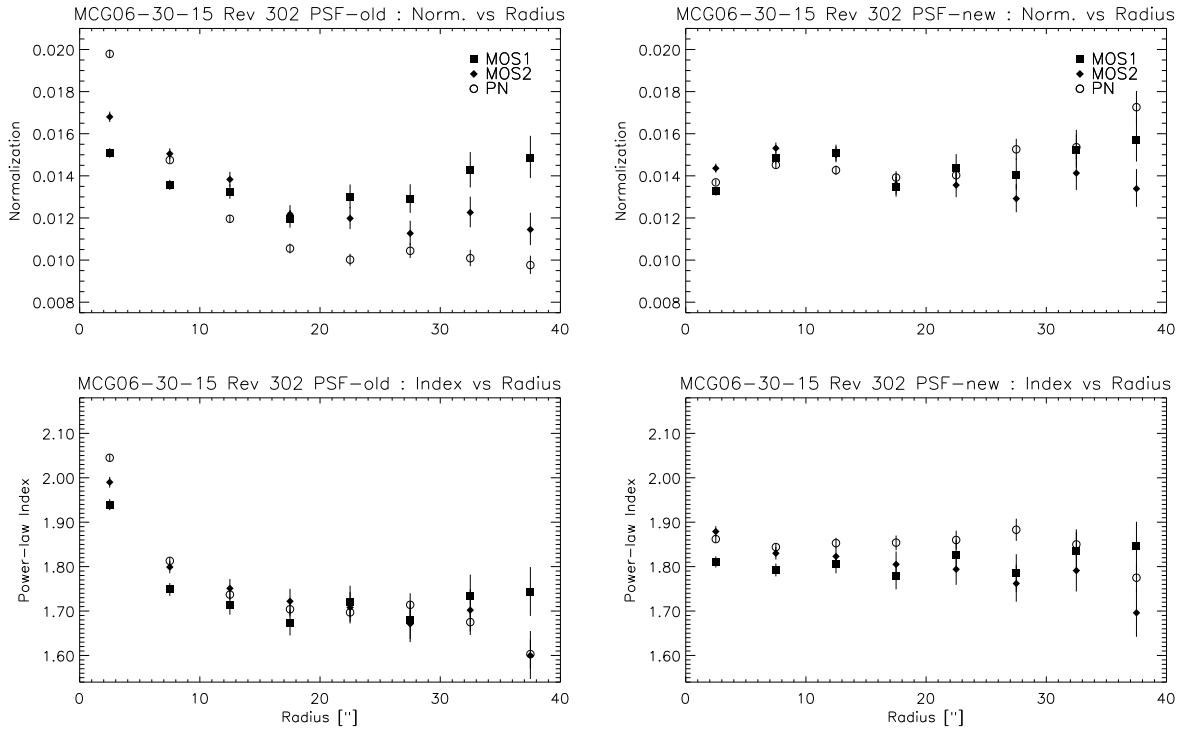

Figure 3: Plots showing how the fitted normalization (top) and power-law index (bottom) vary as a function of extraction 'radius' (see text), using the current CCF PSFs (left) and the new CCF PSFs (right) for the MCG-06-30-15 Rev. 302 data.

the equivalent plots, this time using the Ark120 Rev. 679 data. Again, a very significant improvement is seen with the new PSFs.

4 Estimated Scientific Quality

A major problem with the previous parameterisation was its inability to produce consistent spectral fits for annular extraction regions such as are used for the analysis of piled-up sources. To quantify the improvement with the new PSFs over the old PSFs, MCG-6-30-15 (from Rev 302) has been extracted from annuli of 5-40″, 10-50″and 15-60′ ′and fits compared to those of a circular extraction (0-30″). This has been performed using the new and the old PSFs, and the results are presented in Fig.5. Whereas usage of the old PSFs results in a per instrument normalization variation of up to 40%, and changes in the fitted spectra slope of 0.2, the new PSFs give rise to normalization variations of nearer 5% and a spectral slope change of at most 0.03.

As yet, no sources bright enough for this type of analysis to be performed off-axis have been observed. Indeed, as very long observations in small window mode are necessary, and as small window mode can only be accessed close to on-axis, then the situation may remain like this. As such, the general off-axis results of previous work [1, 2, 3] have been used to transform the new on-axis parameters presented here to projected off-axis values.

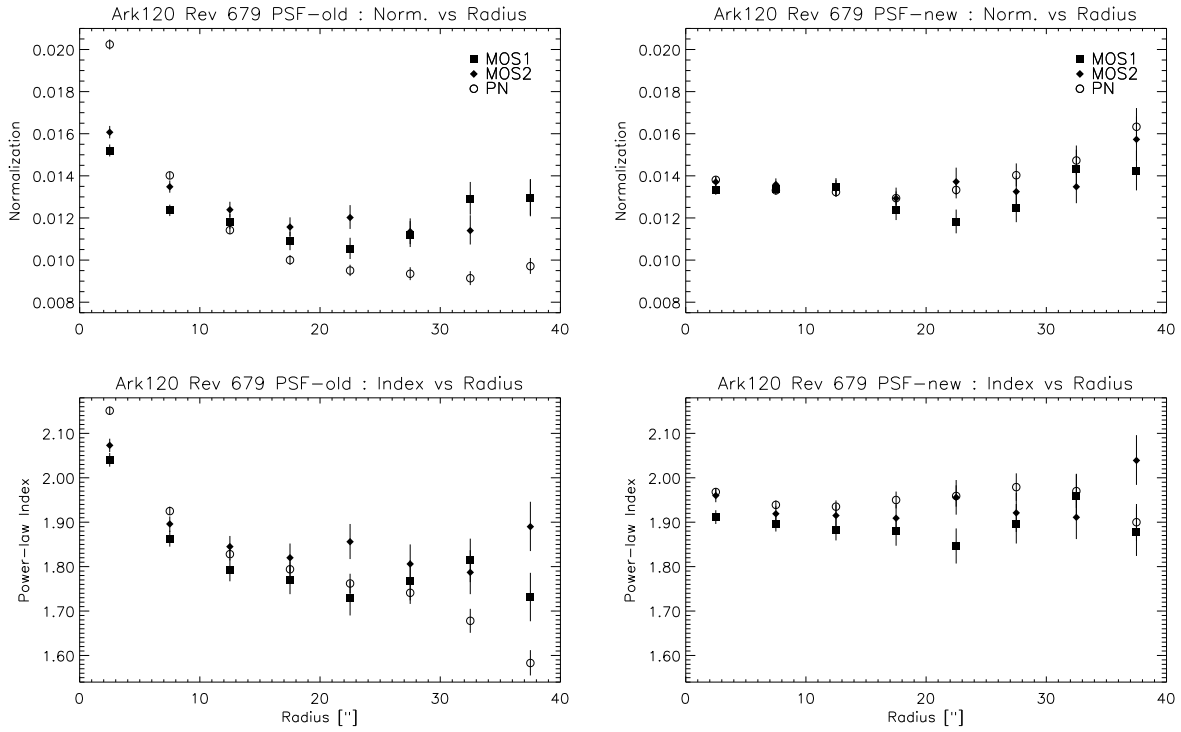

Figure 4: Plots showing how the fitted normalization (top) and power-law index (bottom) vary as a function of extraction 'radius' (see text), using the current CCF PSFs (left) and the new CCF PSFs (right) for the Ark120 Rev 679. data.

5 Expected Updates

None are foreseen as regards revising the King parameterization of the PSFs.

6 Test procedures and Results

The changes introduced here directly affect the encircled energy correction which is applied by the SAS task `arfgen`. The analysis detailed in sections 3 and 4 has used arfgen version 1.65.11 (SAS 6.0) in conjunction with the new PSF CCFs.

References

[1] S. Ghizzardi, "In-flight calibration of the on-axis and near off-axis PSF for the Mos-1 and Mos-2 cameras", EPIC-MCT-TN-011.

[2] S. Ghizzardi, "In-flight calibration of the PSF for the pn camera", EPIC-MCT-TN-012

[3] R.D. Saxton, "PSF of the X-ray telescopes", XMM-CCF-REL-116

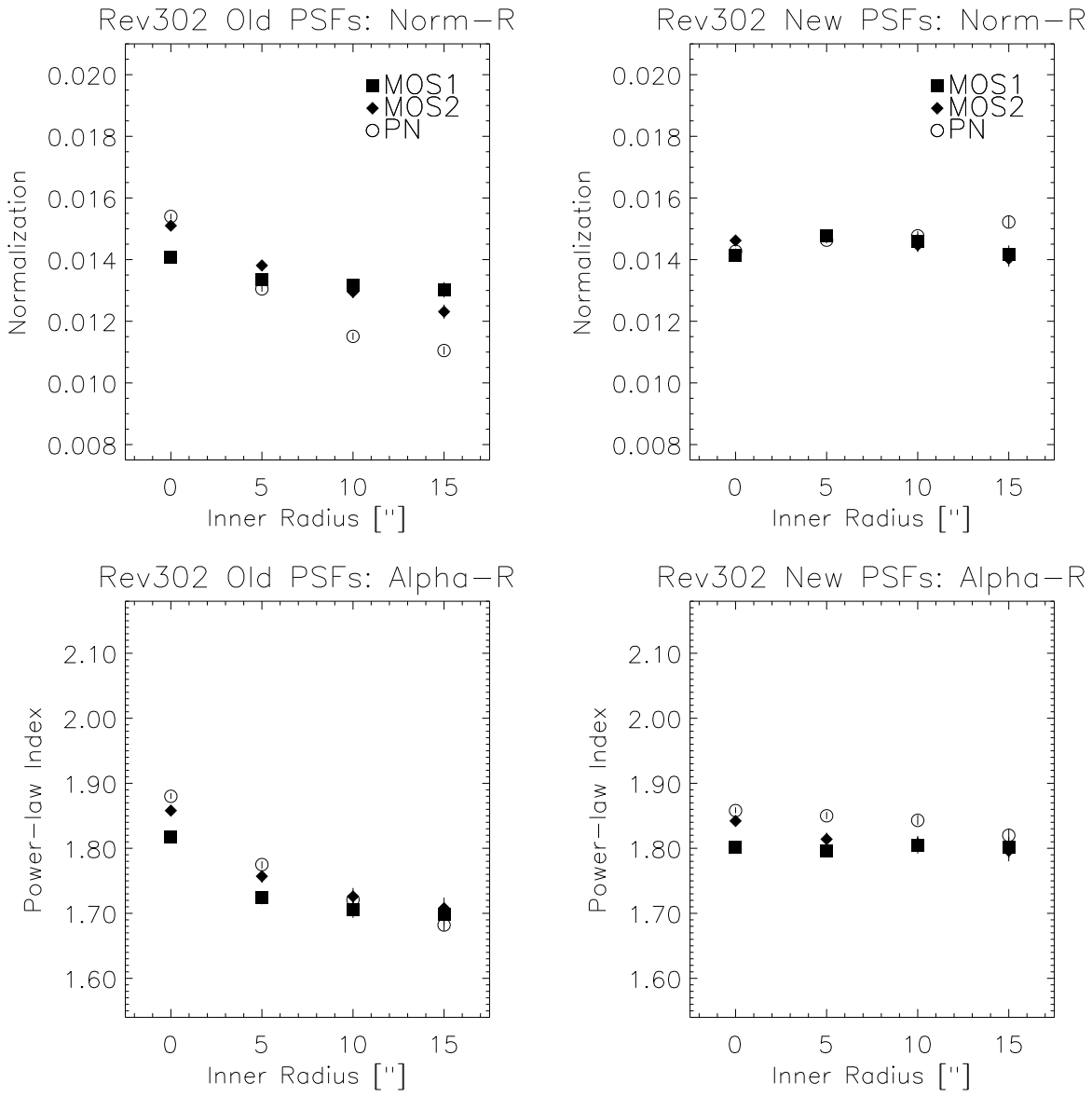

Figure 5: Plots showing how the fitted normalization (top) and power-law index (bottom) vary as a function of extraction region (left to right: 0-30" circle, 5-40" annulus, 10-50" annulus, 15-60" annulus), using the current CCF PSFs (left) and the new CCF PSFs (right) for the MCG-06-30-15 Rev.302 data.